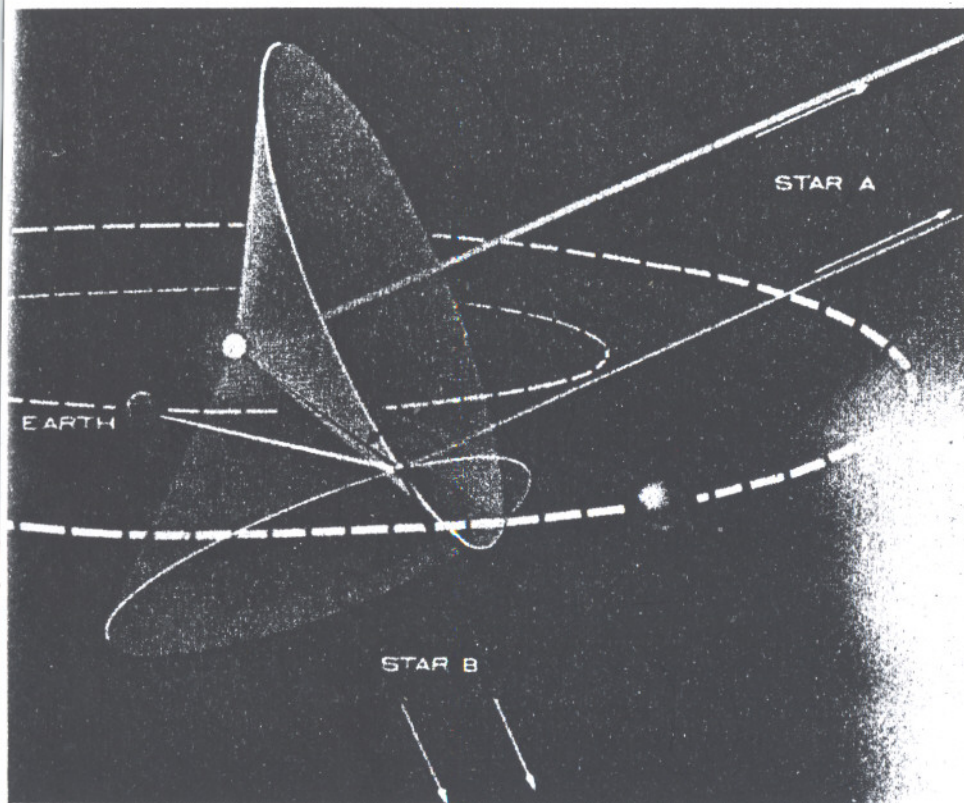


Astronautical guidance

Richard H. Battin

Deputy Associate Director
Instrumentation Laboratory
Massachusetts Institute of Technology



Frontispiece Geometry of fix in space

McGraw-Hill Book Company
New York San Francisco Toronto London

1964

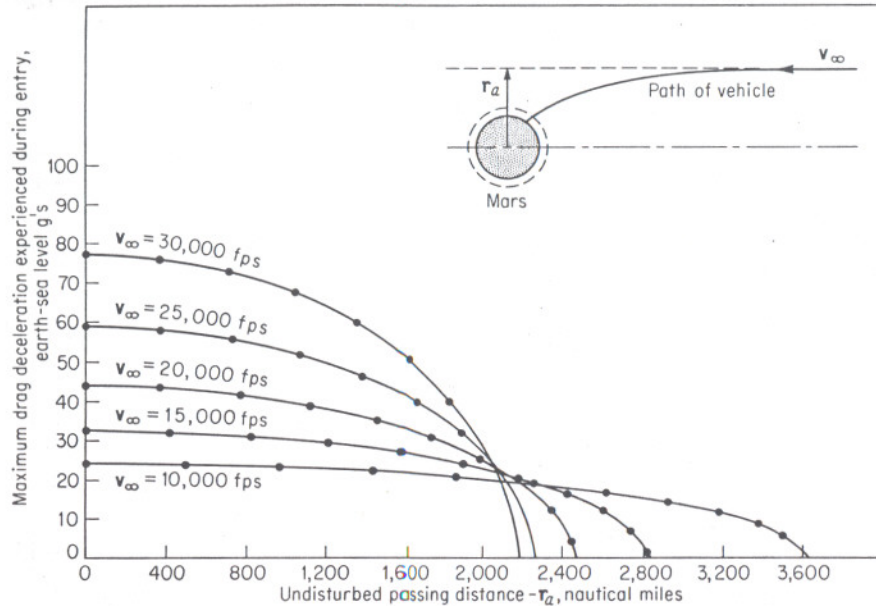


Figure 5.23 Maximum drag deceleration during entry into Martian atmosphere.

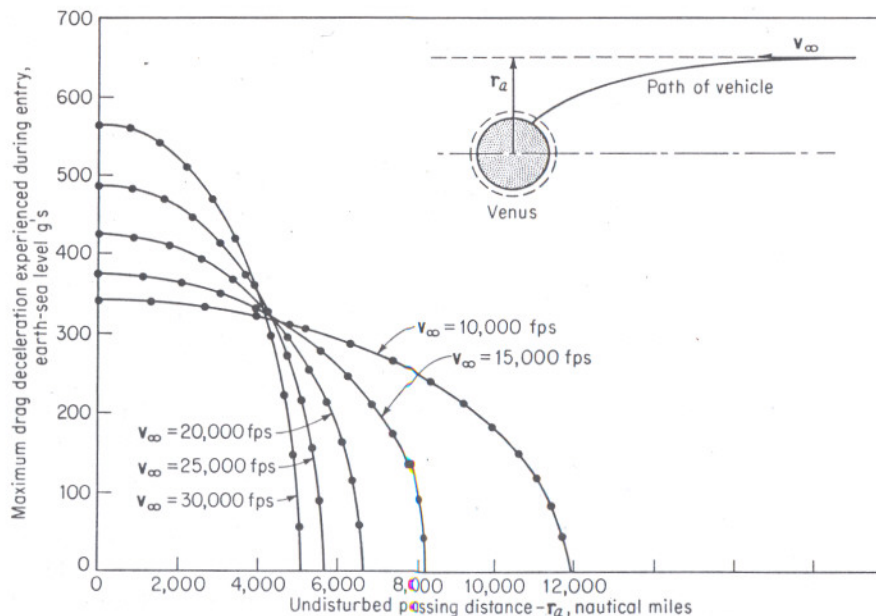


Figure 5.24 Maximum drag deceleration during entry into Venusian atmosphere.

shown curves of the maximum deceleration as a function of the undisturbed passing distance r_a for various values of the relative approach velocity for Mars and Venus.

Here again the virtues of the slow approach are self-evident. The tolerances on guidance accuracy for a specified upper bound on drag deceleration are considerably relaxed for the slow-approach trajectory. For example, with an approach velocity of 10,000 fps and a maximum drag limit of 10 g's, a variation of approximately 100 miles about an r_a of 3,500 miles can be tolerated. If the approach velocity increases to 15,000 fps, the allowed variation is reduced by more than a factor of 2 for the same deceleration limits. On the other hand, the drag deceleration curves of Fig. 5.24 present a most discouraging picture for a probe of the Venusian atmosphere or a soft landing. The allowable tolerances are at least an order of magnitude more severe than the corresponding problem for Mars.

5.4 Round-trip interplanetary reconnaissance trajectories

Consider as a specific mission for an interplanetary voyage placing a spacecraft in an orbit that passes within a few thousand miles of another planet and subsequently returns to earth. The problem of determining a suitable one-way trajectory has been discussed in Sec. 5.2. The added complication of requiring the vehicle to return to earth without additional propulsion (except that needed to correct for navigation inaccuracies) would not contribute significantly to the difficulty of obtaining a solution were it not for the deflection of the orbit caused by the gravitation field of the planet as the spacecraft passes. However, with the material developed in the previous two sections as background, a computation procedure needed to determine round-trip, nonstop, free-fall interplanetary trajectories may be formulated as follows.

The outbound portion of the round-trip trajectory is determined as for the one-way case. The spacecraft velocity vector can then be calculated, and the velocity relative to the destination planet determined. Since the gravitation field of the planet can only rotate this velocity vector, the spacecraft must leave the planet for a return trip to earth with a known relative velocity and at a known time. The problem of establishing a return trajectory is solved basically by an iteration. The procedure consists of making, and systematically revising, an estimate of the time required for the return trip. For each such estimate a new trajectory is calculated until one is obtained which matches the relative-velocity magnitude at the target planet.

It is, of course, possible that no return path exists corresponding to the required departure time and the relative-velocity magnitude. However, when a matching pair of trajectories, outbound and return, has been found, one final step remains. It is necessary to determine if the velocity change

at the destination planet can be effected during the period of contact solely by the planet's gravitation. The required turn angle 2ν is readily computed from the inbound and outbound relative velocity vectors. Thus

$$\sin 2\nu = \frac{|\mathbf{v}_{\infty o} \times \mathbf{v}_{\infty i}|}{v_{\infty}^2} \quad (5.7)$$

The minimum passing distance can then be determined from

$$r_m = \frac{\mu(\csc \nu - 1)}{v_{\infty}^2} \quad (5.8)$$

If r_m is of reasonable magnitude, the solution is complete and a satisfactory round-trip path has been found.

The simplest possible round-trip trajectory would be an orbit whose period is a multiple of the earth's period. Consider first the possibilities of a spacecraft orbit with a period of 1 year which intersects the orbits of both earth and the destination planet. It is shown in Prob. 5.2 that the minimum required departure velocity for a Mars mission is more than 50,000 fps after the vehicle has escaped from the earth's gravitational field. However, for the Venus trip, the short outbound time of flight and the large gravitational pull together make possible conditions which more nearly approximate those required for a 1 year round-trip trajectory. Normally, the period of the outbound orbit will be slightly less than 0.8 year while the return path will have a period of approximately 1 year. A typical round trip requires roughly 1.2 years, of which about 0.4 year is spent from earth to Venus and 0.8 year in return.

With the severe propulsion requirements ruling out the 1-year round-trip to Mars, an alternate possibility is a space vehicle orbit with a 2-year period. An example of such a trajectory is presented in Fig. 5.25.

The departure velocity for the Mars trajectory is 18,200 fps after escape, and 1.5293 years are required for the outbound trip. After passing 7,892 miles from the surface with a relative excess hyperbolic velocity of 28,852 fps, the vehicle returns to earth 0.3673 year after contact.

The 2-year Mars trajectory class divides naturally into two categories. For the one illustrated in Fig. 5.25, contact is made on the second crossing of the Martian orbit. By launching a few months earlier, a 2-year round trip may be achieved for which contact is made on the first crossing. As a specific example for this case, the vehicle is launched on November 6, 1962, with a departure velocity of 18,500 fps. After 0.3985 year the vehicle passes 4,041 miles from the Martian surface with a relative excess hyperbolic velocity of 32,282 fps and then returns to earth 1.6957 years after contact.

Unfortunately, the 2-year round-trip to Mars has a somewhat tight

restriction with respect to times of launch. Although we may expect this class of trajectories approximately to recur with the Martian synodical period of 780 days, the duration of the period for favorable launch conditions with reasonable velocities and passing conditions at Mars is roughly one month.

The tolerances on the 1-year Venus and the 3-year Mars trajectories are much less severe. For the 3-year Martian reconnaissance trajectory,

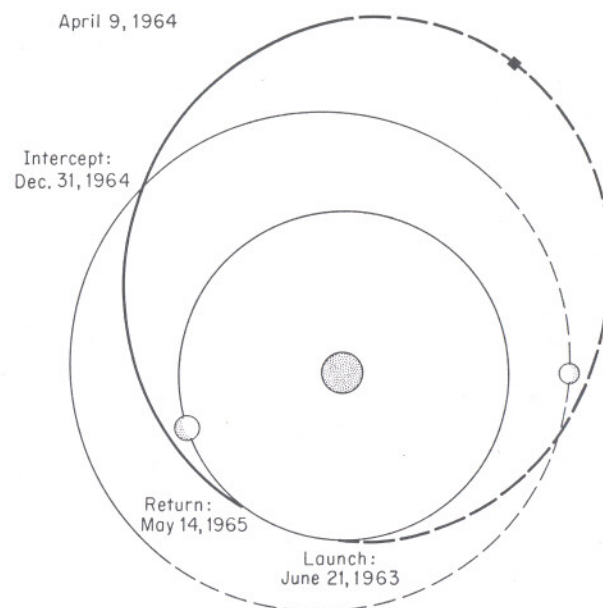


Figure 5.25 Two-year Martian reconnaissance trajectory.

the space vehicle makes two circuits about the sun while the earth makes three. Thus, either the earth to Mars trajectory or the return trajectory, but not both, will be characterized by a heliocentric angle of travel which exceeds a full revolution.

A partial survey of these classes of round-trip trajectories, which have launch dates in the years 1962–1963, has been made. A part of these data is presented graphically in Figs. 5.26 to 5.29 and is catalogued according to certain pertinent geometric features. For the sake of brevity, the graphical data are confined to those trajectories which take the direct path to Mars and the indirect return.

A two-digit category number is used with the right-hand digit associated with the earth-to-planet paths and the left-hand digit with the return path. From the category number, one can determine the sign of the radial

component of the velocity vector of the spacecraft at the points of launch, arrival, and return, together with the number of complete circuits of the sun which the vehicle makes on either leg of the journey. The terminology *radially out* at departure or destination is used when the radial velocity component is positive and *radially in* when it is negative. The code is given in Table 5.4. For example, trajectory category number 53 would be radially in at launch and arrival and the vehicle would traverse a heliocentric angle θ of less than 360° for the first leg of the trip. Then, on the return path, the spacecraft would be radially in at departure, make more than one complete circuit of the sun ($\theta > 360^\circ$), and be radially out on return to earth.

In the figures are shown curves of the passing distance as a function

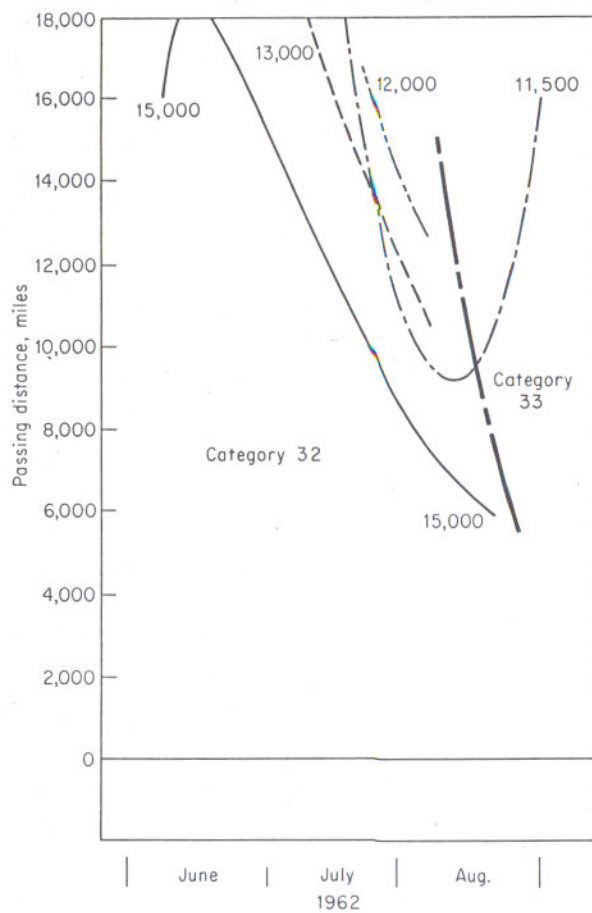


Figure 5.26 Passing distance at Venus versus departure date.

Table 5.4 Trajectory categories for round-trip reconnaissance

Digit code	Departure	Destination	No. of circuits
0	Radially out	Radially out	0
1	Radially in	Radially out	0
2	Radially out	Radially in	0
3	Radially in	Radially in	0
4	Radially out	Radially out	1
5	Radially in	Radially out	1
6	Radially out	Radially in	1
7	Radially in	Radially in	1

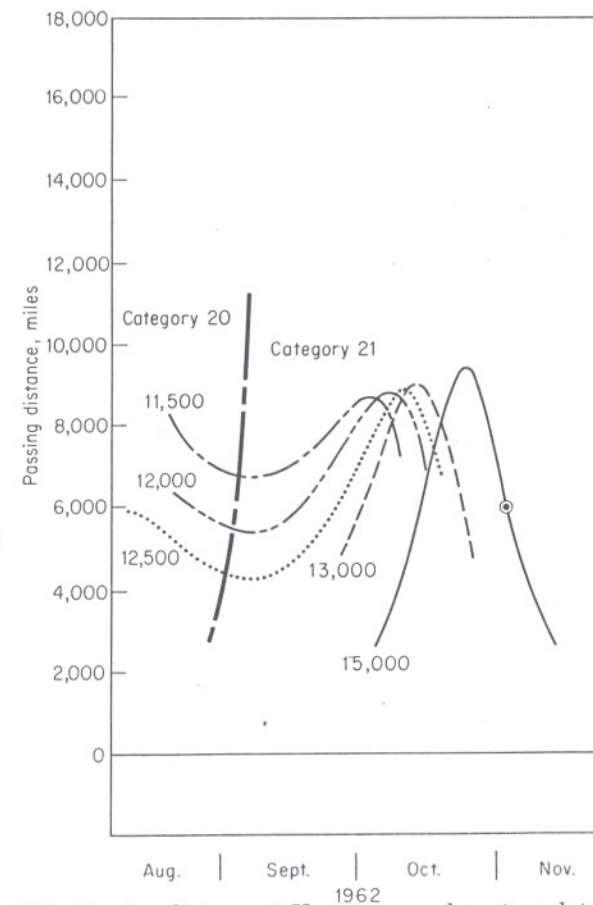


Figure 5.27 Passing distance at Venus versus departure date.

of departure date for various values of the departure velocity. Figures 5.26 and 5.27 describe the Venus trajectories, while Figs. 5.28 and 5.29 are for Mars. The heavy lines in the graphs serve to separate categories and may be thought of as the loci of trajectories with zero radial velocity at launch.

Consider first the Venus trajectories. Early in June round-trip solutions of the type 32 are possible for a departure velocity of 15,000 fps. As seen in Fig. 5.26 the curve peaks in the middle of June. At this same time the angle θ is passing through 180° , which, from earlier discussions, is known to be a critical value. Solutions continue to exist throughout the months of July and August, and it is seen in the case of 11,500 fps departure velocity that the curve has a minimum near the middle of August.

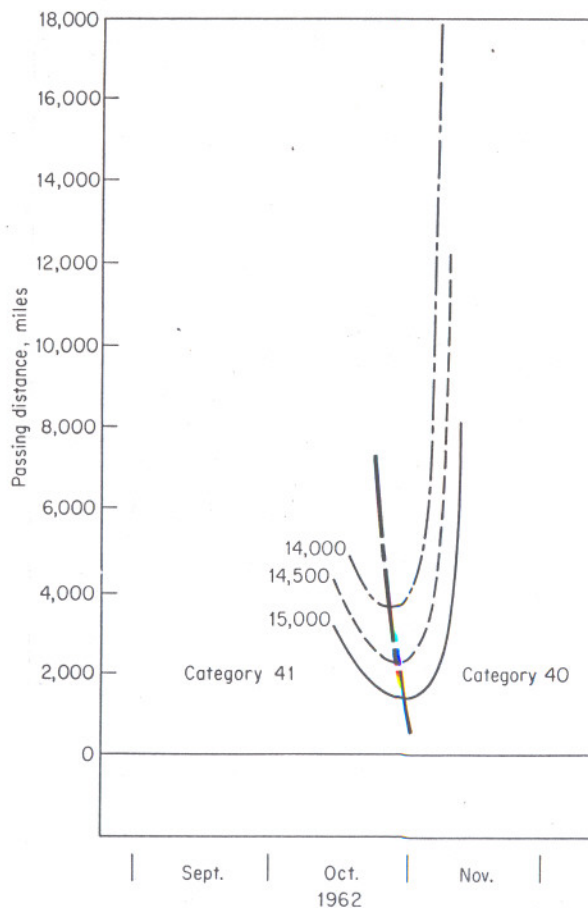


Figure 5.28 Passing distance at Mars versus departure date.

At about the same time the category changes from type 32 to 33, and at transition the vehicle is launched tangent to the earth's orbit. This particular effect—the vanishing of the radial component of launch velocity occurring near the minimum in the passing distance curve—seems to be characteristic of all the curves for both Venus and Mars.

As another point of interest, note that these curves frequently cross one another, thereby demonstrating the possibility of achieving identical passing distances at the destination planet with two spacecrafts launched on the same day but with different velocities.

Another striking characteristic of the Venus trip solutions is that they all require essentially the same time for a round trip, namely, 1.2 years, with

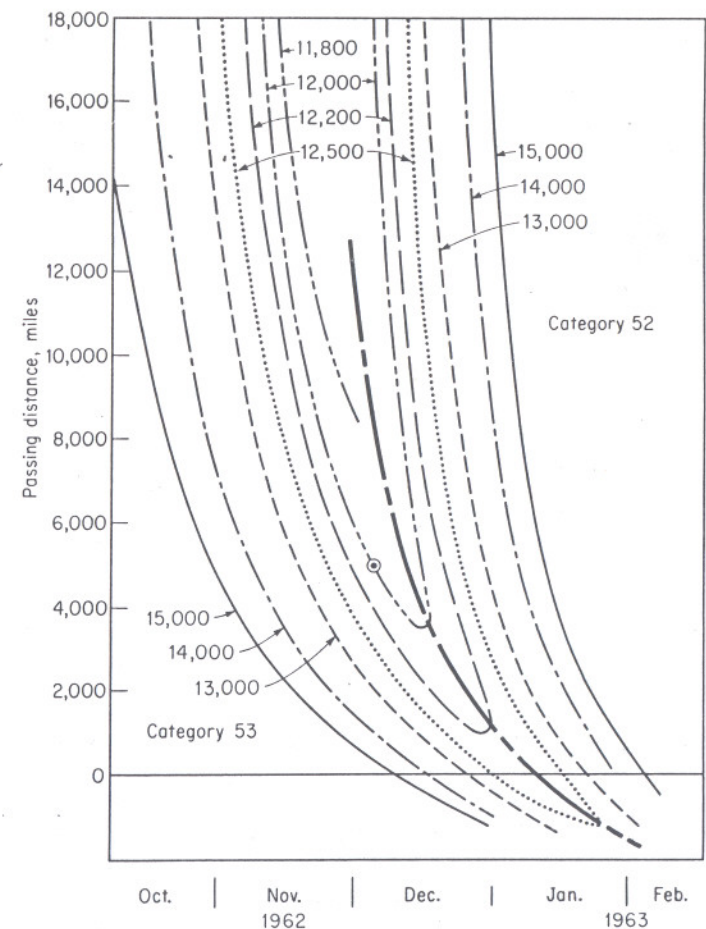


Figure 5.29 Passing distance at Mars versus departure date.

Feb. 20, 1963

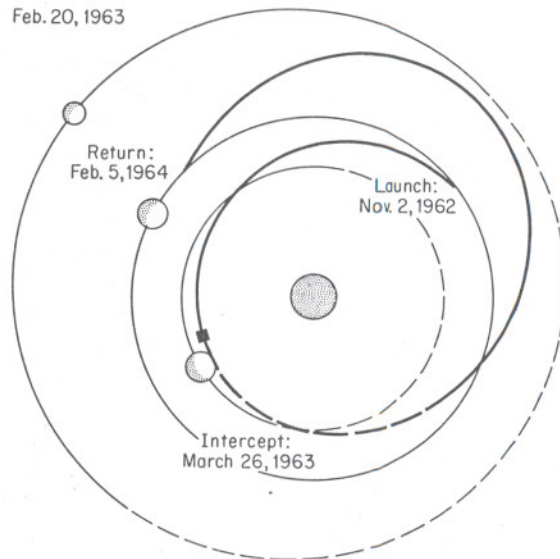


Figure 5.30 Venusian reconnaissance trajectory, category 21.

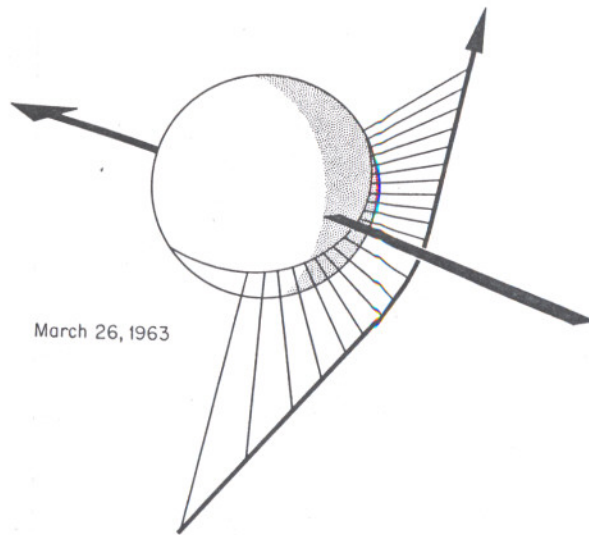


Figure 5.31 Orientation during Venusian contact, category 21.

a return-trip time approximately twice that for the outbound leg. The same type of phenomenon is observed for the Mars solutions in that the round-trip time is approximately 3.1 to 3.2 years.

Turning now to the Mars curves, it is seen from Fig. 5.28 that practical solutions are possible in categories 41 and 40 for October and early in November. At the same time, from Fig. 5.29, trajectories in category 53

are also possible. These, in turn, persist throughout November and most of December when the passing distances become negative for the larger velocities. During this period the value of θ is passing through 180° .

As launch time increases, each of the constant-velocity curves of Fig. 5.29 reaches a minimum and the category changes from 53 to 52. A most interesting phenomenon is observed here—the curves double back on themselves. Thus, on the same date of departure and with the same velocity magnitude, one may launch radially out or radially in to obtain a round-trip solution each having a different passing distance.

A typical round-trip Venusian reconnaissance trajectory is illustrated in Fig. 5.30. A small spot on the graph of Fig. 5.27 serves to locate the trajectory in context with the other possibilities. For the example shown, the vehicle velocity relative to earth after escape is 15,000 fps. After 0.3940 year the spacecraft passes 5,932 miles from the surface of the planet with a relative approach velocity of 25,100 fps and returns to earth 0.8635 year later, entering the atmosphere with a velocity of 50,738 fps. The motion of the space vehicle relative to Venus during the period of contact is illustrated in Fig. 5.31. The direction of motion of the planet is shown, together with the hyperbolic contact trajectory of the spacecraft.

The trajectory chosen to illustrate the 3-year round-trip Martian reconnaissance mission is located by the small spot in Fig. 5.29. The earth-to-Mars orbit is shown in Fig. 5.32, and the return path in Fig. 5.34. The departure velocity is 12,000 fps, and 1.1970 years is consumed to reach Mars. After passing 4,903 miles from the surface with a relative approach velocity of 21,567 fps, the vehicle makes one complete orbit of the sun and returns to earth 1.9131 years after contact with a reentry velocity of 39,921 fps. The relative motion of the spacecraft during planetary contact is shown in Fig. 5.33. In this example, the Martian gravity field has the effect of quadrupling the out-of-plane component of the vehicle velocity and thereby causing a rotation of approximately 30° in the trajectory line of nodes.

For comparative purposes, an example of a trajectory with an indirect route to Mars and a direct return is illustrated in Figs. 5.35 to 5.37. The trajectory, which belongs to the 17 category, has a departure velocity of 15,000 fps and an outbound time of flight of 2.4223 years. After passing 4,693 miles from the surface of Mars with the rather slow approach velocity of 11,390 fps, the vehicle takes 0.8006 year to return to earth. It is interesting to compare the geometry of the relative motion during contact with Mars as shown in Fig. 5.36 with the previous example illustrated in Fig. 5.33.

Returning momentarily to the Venusian reconnaissance trajectory shown in Fig. 5.30, it is of interest to note that the increased velocity introduced at Venus is sufficient to carry the spacecraft on the return trip to a distance of about 1.35 astronomical units from the sun. Since Mars at perihelion is

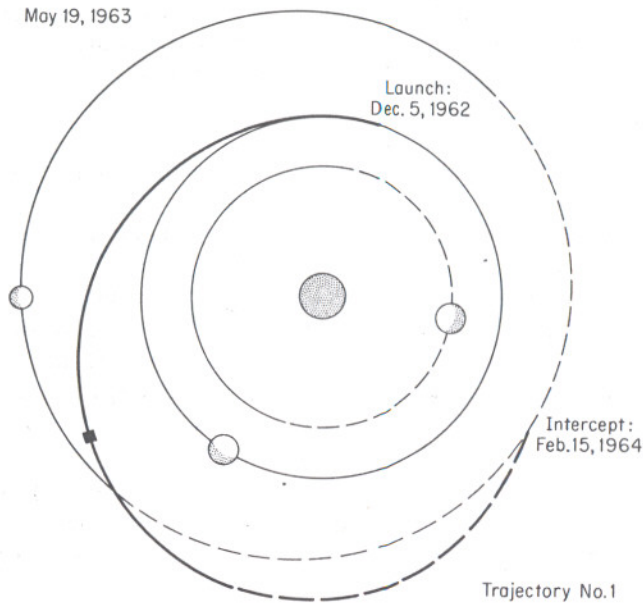


Figure 5.32 Three-year Martian reconnaissance trajectory, category 53—outbound.

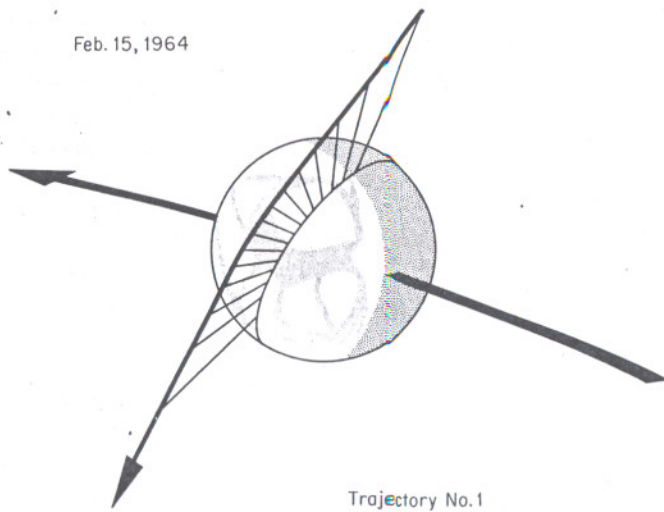


Figure 5.33 Orientation during Martian contact, category 53.

only at a distance of 1.38 astronomical units, the interesting possibility arises of a dual contact with both planets and a total time of flight for the round trip just in excess of 1 year. This would clearly be an improvement over the 3.2-year round trip to Mars alone. The principal drawback to such a double reconnaissance is the infrequency of possible launch dates. The synodical periods for Venus and Mars are 584 and 780 days, respectively. Therefore, one can expect favorable conditions for round-trip missions to each planet individually to recur with the corresponding synodical

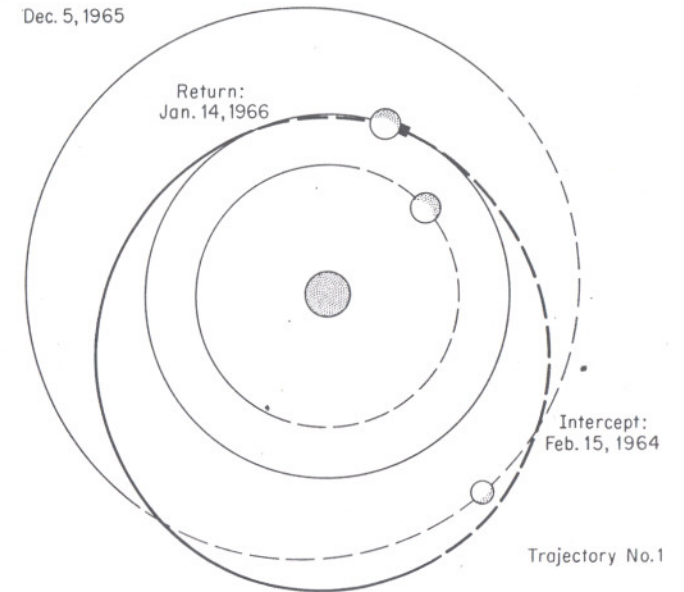


Figure 5.34 Three-year Martian reconnaissance trajectory, category 53—return.

frequency. On the other hand, roughly 2,340 days are required before any particular configuration of the three planets, earth, Venus, and Mars, will be approximately repeated. Even then the likelihood of a configuration existing at all in the near future which would admit of the dual mission seems remote.

Nevertheless, on June 9, 1972, the ideal circumstances prevail. On that date a vehicle in a parking orbit from Cape Kennedy on the 110° launch azimuth course may be injected into just such a trajectory at the geographical location of 5° west and 18° south and with an injection velocity of 39,122 fps. After escape the vehicle will have a velocity relative to the earth of 15,000 fps. The first planet encountered will be Venus after a trip lasting 0.4308 year. The vehicle will pass 4,426 miles from the surface

Aug. 29, 1963

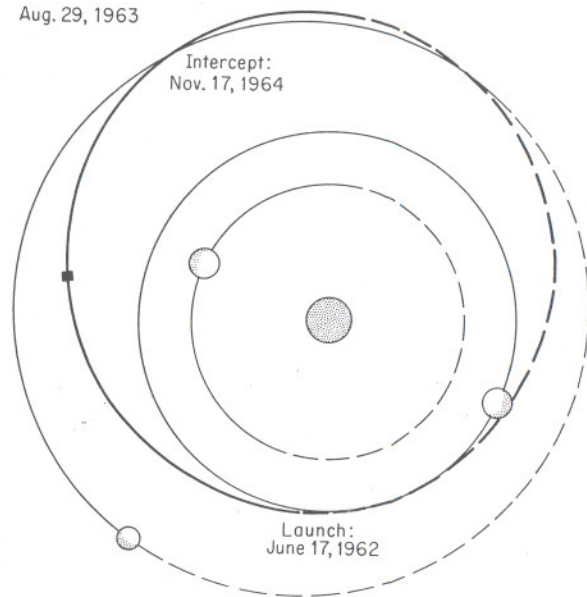


Figure 5.35 Three-year Martian reconnaissance trajectory, category 17—outbound.

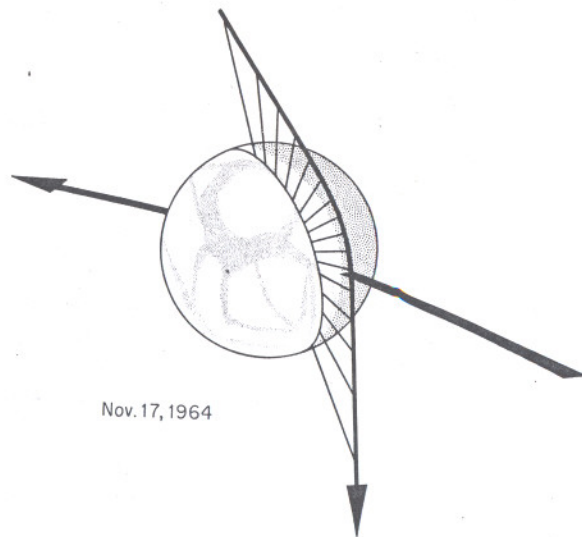


Figure 5.36 Orientation during Martian contact, category 17.

of the planet and will, thereby, receive from the Venusian gravity field alone a velocity impulse sending it in the direction of Mars. The second portion of the trip consumes 0.3949 year, and the spacecraft contacts Mars passing at a minimum distance of 1,538 miles from the surface. The trip from Mars to earth takes an additional 0.4348 year, and the vehicle returns on September 13, 1973. This truly remarkable trajectory is illustrated in Fig. 5.38.

June 25, 1965

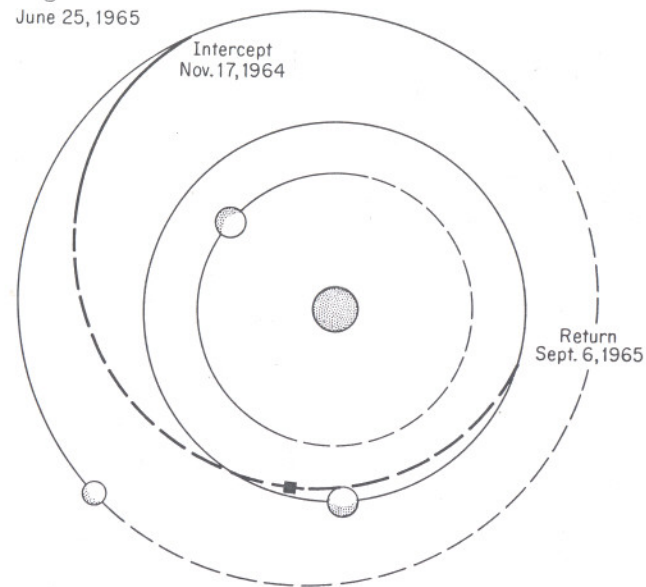


Figure 5.37 Three-year Martian reconnaissance trajectory, category 17—return.

It might be expected from previous remarks that similar conditions would exist approximately $6\frac{1}{2}$ years earlier. Indeed, the trajectory shown in Fig. 5.39 is possible on February 6, 1966, and is similar in all respects but one. With a departure velocity of 16,500 fps the vehicle contacts Venus after 0.4196 year and Mars 0.5454 year later with respective passing distances of 1,616 and 7,515 miles. Now, however, the encounter with Mars occurs quite far from the Martian perihelion. Thus, in order to catch up with the earth, the vehicle must once again pass inside the earth's orbit with the result that the return trip from Mars requires 0.8950 year.

It is sad to report that these double reconnaissance trajectories are little more than astronomical oddities. Unfortunately, the launch-time tolerances appear to be far too severe for them to be exploited with current technology. Unforeseen delays in the countdown of even a few days would necessitate a 6-year postponement in the mission.

June 18, 1973

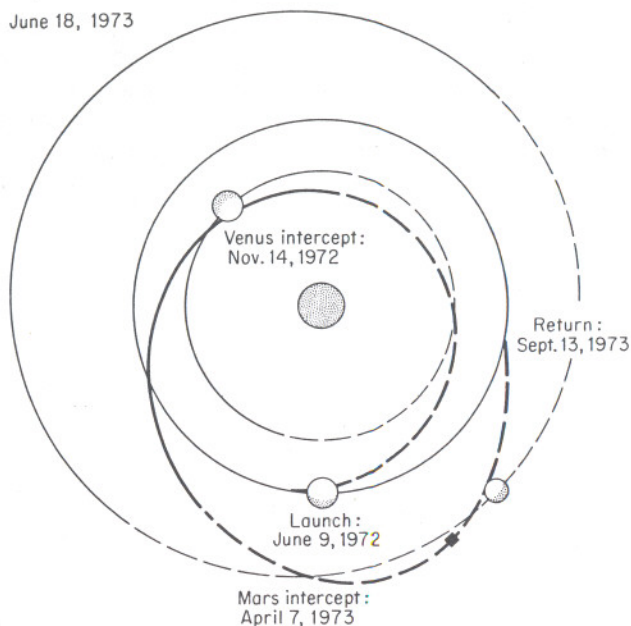


Figure 5.38 Double reconnaissance trajectory.

Sept. 1, 1967

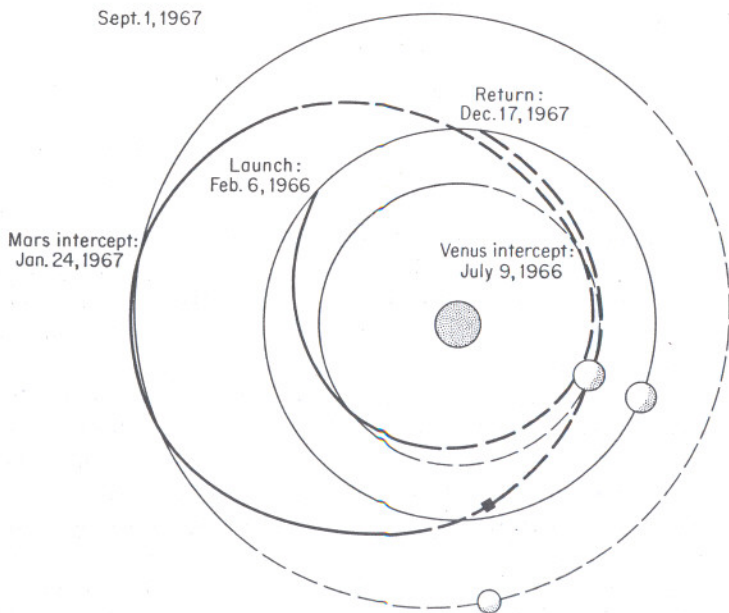


Figure 5.39 Double reconnaissance trajectory.

5.5 Circumlunar trajectories

The motion of a vehicle in cislunar space is governed primarily by the gravitational fields of the earth and moon. The effects of solar gravity and the perturbations arising from the nonspherical shape of the attracting bodies are important in a final analysis but are neglected in obtaining the conic approximation.

The calculation of circumlunar trajectories is more difficult than the corresponding interplanetary problem because the time spent within the lunar sphere of influence is a significant fraction of the total mission time. Thus, it would be out of the question to regard the effect of the moon as simply an impulsive change in the vehicle velocity as was done in the computations of the previous section.

An adequate approximate trajectory may be had by matching in both position and velocity at the junction points (1) an ellipse from earth to the sphere of influence of the moon whose focus is at the center of the earth, (2) a hyperbola around the moon, and (3) an ellipse from the sphere of influence back to earth. The simplified problem, though itself fairly complex, is tractable when the relevant parameters and independent variables are identified. Clearly, an analogous procedure could be used for interplanetary trajectories if it is desired to obtain a better approximation than would result from the simplified treatment described earlier.

In our analysis the following parameters are found to be a convenient choice for the independent variables:

1. r_m , the perilune altitude or minimum passing distance. This parameter is directly related to the total time of flight.
2. t_A , the time of arrival at the sphere of influence of the moon¹ on the outbound trajectory. This is specified as a Julian date. It was decided to fix this time, rather than the time of injection, since the time of flight from injection to the sphere of influence is a parameter which will be varied during the iteration process. Thus, since the position of the moon does not change with time of flight, there is no need during that iteration for continual redetermination of the position of the moon.
3. i_L , the angle of inclination of the outbound trajectory plane with respect to the equatorial plane of the earth. This parameter cannot be freely chosen, since it depends somewhat on the latitude of the launch point. For example, if the parking orbit plane contains the latitude of Cape Kennedy, the inclination angle of the plane cannot be less than this latitude.
4. i_R , the angle of inclination of the return trajectory plane with respect

¹ The actual position of the moon is used in the calculation. It is not necessary to use a simplified model of the moon's orbit.

as the sign of

$$\sin \theta \left[\left(1 - \frac{p}{r_2} \right) r_1 r_2 - \left(1 - \frac{p}{r_1} \right) r_1 \cdot r_2 \right]$$

where p is the parameter of the orbit.

5.6. For the round-trip Mars reconnaissance trajectory illustrated in Figs. 5.32 to 5.34 the approach velocity on return to the earth is given by

$$\mathbf{v}_\infty = 10,619\mathbf{i}_x + 9,682\mathbf{i}_y + 6,493\mathbf{i}_z \quad \text{fps}$$

expressed in a geocentric ecliptic coordinate system. If it desired to impact in the general area of the Gulf of Mexico, compute the magnitude of the point of aim r_a , the incidence angle ψ , and the linear miss ratio defined in Prob. 5.4. The latitude of the Gulf of Mexico may be taken to be 28° .

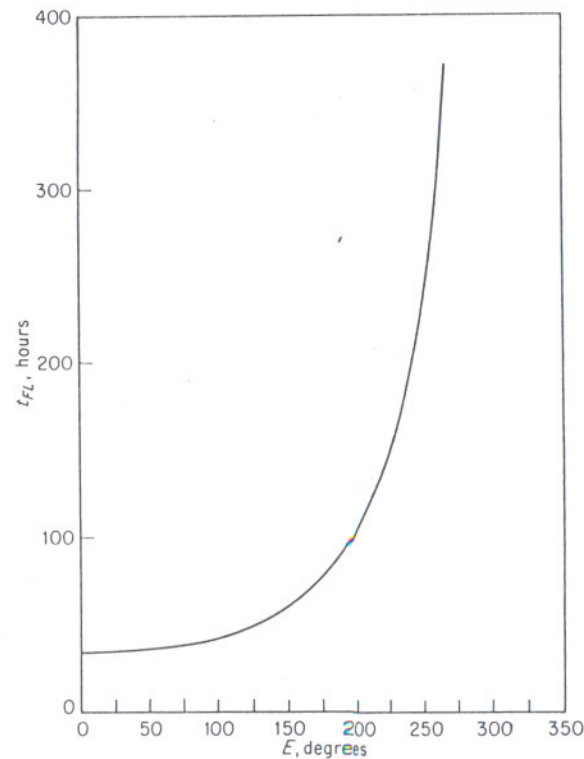


Figure P5.7 Time of flight versus eccentric anomaly.

5.7. For the calculation described in Sec 5.6 it is also possible, for the same purpose, to use Kepler's equation in the form

$$t_{FL} = \sqrt{\frac{a^3}{\mu_E}} \left[E - \left(1 - \frac{r_L}{a} \right) \sin E \right]$$

where E is the eccentric anomaly of the target location r_T . Show that

$$a = \frac{r_T - r_L \cos E}{1 - \cos E}$$

so that

$$t_{FL} = \sqrt{\frac{r_T - r_L \cos E}{\mu_E(1 - \cos E)^3}} [(r_T - r_L \cos E)E - (r_T - r_L) \sin E]$$

gives t_{FL} as a function of the single variable E . Verify that the appropriate derivative needed for the iteration is then

$$\frac{dt_{FL}}{dE} = t_{FL} \left[\frac{1}{2} \frac{r_L \sin E}{r_T - r_L \cos E} + \frac{r_T(1 - \cos E) + r_L E \sin E}{(r_T - r_L \cos E)E - (r_T - r_L) \sin E} - \frac{3}{2} \frac{\sin E}{1 - \cos E} \right]$$

The accompanying figure shows the variation of t_{FL} as a function of E .

Comparison with Fig. 5.45 indicates some possible advantage in using Lambert's time-of-flight expression as opposed to Kepler's form. In the region of interest, the relative insensitivity of t_{FL} as a function of E could lead to some difficulty in obtaining a rapid convergence to the required iterative solution for E .

BIBLIOGRAPHY

The material of this chapter summarizes the research on space trajectories performed at the MIT Instrumentation Laboratory over the past several years. The work on interplanetary trajectories reported here is based on the papers of Laning, Frey, and Trageser (36); Battin (5); and Battin and Laning (11) as well as on certain chapters of two several-volume studies made at MIT (45) and (46).

Sections 5.1, 5.2, and 5.4 were borrowed almost intact from Battin and Laning (11). The one-way interplanetary mission was the subject of the MIT study (46), and the trajectory studies reported therein were performed by Dr. Laning and the author. The graphical plots of drag deceleration during entry into a planetary atmosphere are the work of Mr. Roger Scholten and are from the same MIT study.

Historically, the work on the round-trip interplanetary mission preceded the one-way study and was extensively reported by Laning and Battin in the MIT study (45). Most of the material of Secs. 5.3 and 5.4 is based on that initial study.

The double reconnaissance mission discussed at the end of Sec. 5.4 was originally suggested by Crocco (19). Unfortunately, the Crocco mission requires an excess hyperbolic velocity exceeding 38,000 fps owing principally to the fact that Mars was selected as the first planet to be visited. If the order is reversed and the gravitational field of Venus exploited, the mission can be accomplished with an excess velocity of only 15,000 fps.

The last two sections of the chapter on the subject of circumlunar trajectory calculations are based on the work of Dr. James S. Miller and the present author and were originally reported in their jointly prepared report (13).